RSC Advances

PAPER

View Article Online
View Journal | View Issue

Cite this: *RSC Adv.*, 2018, **8**, 17101

Direct speciation methods to quantify catalytically active species of $AlCl_3$ in glucose isomerization†

Angela M. Norton, Hannah Nguyen, Nicholas L. Xiao and Dionisios G. Vlachos *

Received 11th April 2018
Accepted 25th April 2018

DOI: 10.1039/c8ra03088j

rsc.li/rsc-advances

While homogeneous metal halides have been shown to catalyze glucose to fructose isomerization, direct experimental evidence in support of the catalytically active species remains elusive. Here, we integrate direct speciation methods with kinetics to provide strong evidence for the active species of $AlCl_3$ in glucose–fructose isomerization in water. We investigate the effect of Lewis ($AlCl_3$) and Brønsted (HCl) acids on aluminum hydrolysis and glucose conversion. We demonstrate the interplay between the acids using the Optimum Logic Inc. speciation model (OLI software). We measure aqueous aluminum species and protons through *in situ* and *ex situ* ^{27}Al quantitative nuclear magnetic resonance (qNMR) and pH measurements, respectively, and quantify aluminum nanoparticles through a combination of inductively coupled plasma-mass spectrometry (ICP-MS), dynamic light scattering (DLS), and ultrafiltration. Direct speciation measurements correlated with the glucose isomerization rate indicate that the hydrolyzed Al(III) complex $[Al(H_2O)_4(OH)_2]^{1+}$ is the active species in glucose isomerization.

Introduction

The need to reduce greenhouse gas emissions and our dependence on fossil fuels has prompted considerable research in the production of fuels and chemicals from lignocellulosic biomass.[1] Biomass is a promising renewable feedstock due to its abundance and its ability to capture CO_2 from the atmosphere *via* photosynthesis.[2] Among the top biomass-derived chemicals, 5-(hydroxymethyl)furfural (HMF) has gained significant interest as a platform chemical.[2] HMF synthesis results from the hydrolysis of cellulosic biomass to glucose, glucose isomerization to fructose, and fructose dehydration to HMF.[1] When the isomerization and dehydration steps occur in a single pot, dehydration drives the equilibrium-limited isomerization resulting in higher yields.[3] This then requires an isomerization catalyst that is compatible with the Brønsted acid catalyst and high temperatures associated with the dehydration reaction. Currently, industrial applications use immobilized D-xylose ketoisomerase to catalyze the isomerization;[4,5] however, these catalysts are expensive, operate under narrow conditions, and require highly pure glucose.[6] As a result, research has turned to the development of chemo-catalytic processes to carry out glucose isomerization, starting with the pioneering work of Davis and co-workers on Sn-BEA zeolite that enable HMF production in a single pot.[7,8]

Metal halides are related homogeneous chemo-catalysts.[3,9–12] Hu and co-workers compared the catalytic activity of $AlCl_3$, $CrCl_3$, and $SnCl_4$ and found that $CrCl_3$ exhibits the highest initial turnover frequency (TOF), while $AlCl_3$ is the most selective catalyst to fructose.[9] Mechanistic studies of glucose isomerization with $AlCl_3$ and $CrCl_3$ show that the isomerization proceeds through a 1,2 hydride transfer, and this step is rate-limiting according to kinetic-isotope effect measurements.[3] Based on theoretical investigations,[13] the catalytic species responsible for the isomerization likely exists as a bifunctional Lewis acidic/Brønsted base site, in which the Brønsted base (–OH) facilitates an initial proton transfer, activating the subsequent Lewis acid (metal center, M) catalyzed C2 → C1 hydride shift (Scheme 1).[10] Direct experimental evidence in support of the catalytic species has though been lacking. This lack of understanding stems from a number of metal hydrolysis steps and self-condensation leading to oligomeric species and potentially metal nanoparticles.[14–16]

Different approaches have emerged to identify the catalytically active species. Our group combined kinetic rate measurements with a speciation thermodynamic model, called Optimum Logic Inc. Systems' Stream Analyzer software (OLI software, 2017), to suggest $[Cr(H_2O)_5(OH)]^{2+}$ is active in $CrCl_3$-catalyzed glucose isomerization.[17] Hu and co-workers performed tandem electrospray ionization mass spectrometry (ESI-MS/MS) to propose, due to its abundance, $[Al(H_2O)_4(OH)_2]^{1+}$ is the active species when $AlCl_3$ is used as a catalyst.[9,18] Given the difference in the active species between $CrCl_3$ and $AlCl_3$, the fact that ESI-MS/MS may alter speciation during the measurement,[19] and that observed species are often spectators rather than the

Catalysis Center for Energy Innovation, Department of Chemical and Biomolecular Engineering, University of Delaware, 221 Academy St., Newark, DE 19716, USA. E-mail: vlachos@udel.edu

† Electronic supplementary information (ESI) available. See DOI: 10.1039/c8ra03088j

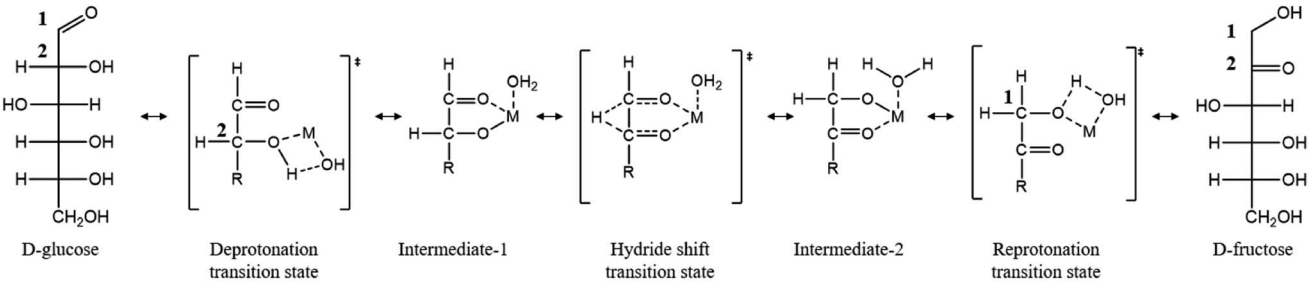

Scheme 1 Proposed mechanism of glucose to fructose isomerization in water. "M" represents a metal center [*e.g.*, Cr, Al, and Sn (in Sn BEA)]. Redrawn from ref. 3.

active ones, the active aluminum species still remain(s) unknown.

In this work, we integrate kinetics with more direct speciation measurements for the first time to provide evidence for the active species of $AlCl_3$. Our judicious choice of $AlCl_3$ is based on the fact that it is a selective catalyst in glucose isomerization and an excellent salt to be followed spectroscopically.[20–24] We investigate the interplay between Lewis ($AlCl_3$) and Brønsted (HCl) acids using the OLI software, while simultaneously developing an experimental protocol to quantify the various aluminum species. We use ^{27}Al quantitative nuclear magnetic resonance (qNMR) and pH to measure the aqueous aluminum species and protons, respectively, and combine inductively coupled plasma-mass spectrometry (ICP-MS), dynamic light scattering (DLS), and ultrafiltration to measure the aluminum nanoparticles. Finally, we correlate the glucose isomerization rate with the aluminum species' concentrations to propose an active species.

Methods

Speciation model

$AlCl_3$ speciation was predicted using the mixed-solvent electrolyte OLI software.[25,26] The model predicts speciation by solving chemical equilibria of multicomponent systems and combining standard-state thermochemical properties of solution species with an expression for the excess Gibbs free energy. The standard-state properties are calculated using the Helgeson–Kirkham–Flowers (HKF) equation of state for aqueous ions and electrolytes at infinite dilution, while the excess Gibbs free energy model incorporates short, middle, and long-range electrostatic interactions. Further details regarding these calculations can be found in our previous work.[8] The OLI model has been parameterized at conditions that differ from those typically encountered in isomerization chemistry and thus, its accuracy is unknown. We address this point in this paper by more direct measurements of aluminum speciation.

pH measurements

pH measurements were obtained using the 3300 High Temperature (HT) PERpH-X sensor (Rosemount) and the 56 Advanced Dual-Input analyzer (Rosemount). A typical measurement was conducted in a 100 mL thick-walled glass vessel (Fisher Scientific) containing catalyst solution. The catalyst solution was stirred and heated for a specified time. The pH sensor was then inserted into the vessel and pH was obtained *in situ*. Heated samples were then cooled to room temperature and pH was obtained *ex situ*. The sensor was confirmed to measure the pH of buffer solutions (Fisher Scientific) within their specified temperature range (298 to 373 K, see Fig. S1†).

^{27}Al qNMR spectroscopy

^{27}Al qNMR was carried out on an Avance III 400 MHz NMR spectrometer (Bruker). Spectra were measured at 104.27 MHz (pulse width: 12.50 μs, acquisition time: 0.1966 s, scans: 64, solvent: 90% H_2O, 10% D_2O) and processed using Mestrelab Research software (mNOVA). The samples were prepared in quartz NMR tubes (NewEra), containing 0.5 mL of reaction mixture and were studied at 303 or 363 K. For quantification purposes, an external standard of $Al(H_2O)_6^{3+}$ was prepared with 5 mM $AlCl_3$ and 100 mM HCl (Fig. S2†).

Ultrafiltration

Ultrafiltration was performed using Vivaspin 500 concentrators (Sartorius) with a 10 000 molecular weight cut-off (MWCO). The concentrators were filled with 500 μL of either freshly prepared or heat-treated catalyst solutions and placed into the centrifuge (Eppendorf Centrifuge 5424) for 15 minutes at a spin speed of 15 000*g*. Samples were then recovered from the bottom of the concentrate pocket with a pipette.

ICP-MS

ICP-MS measurements on freshly prepared and heat-treated catalyst solutions were carried out using an Agilent 7500cx Series instrument (Wilmington, DE). Samples underwent ultrafiltration, followed by acid treatment prior to ICP-MS analysis. The aluminum standards (Agilent) were prepared in HNO_3 (70 w/w%, Sigma Aldrich) and diluted for the ICP-MS calibration.

DLS

DLS experiments were conducted on a Brookhaven ZETAPALS instrument. DLS measurements were obtained both before and after heating the catalyst solutions. The autocorrelation functions were analyzed using the Multimodal Size Distribution

algorithm of the accompanying software, where the viscosity of the solutions was assumed to equal that of water.

Catalytic measurements

All chemicals were purchased from Sigma Aldrich and used as received. The reactions were conducted in 10 mL glass vials (Sigma Aldrich) heated in an aluminum reactor block with controlled stirring (Fisher Scientific). Catalyst solutions of $AlCl_3 \cdot 6H_2O$ (Sigma Aldrich) and HCl (37 w/w%, Sigma Aldrich) were stirred and preheated at reaction temperature for 24 h. Kinetic experiments were then carried out in sealed reactor vials containing the preheated catalyst solution (2 mL) and glucose. The Al-to-reactant molar ratio was kept at 9 : 100, which corresponds to 5 mM $AlCl_3$ and 1 wt% glucose solution. The HCl concentration varied from 3 to 44 mM when used with $AlCl_3$ (except for the external standard mentioned above). At different time points, the vials were removed from the oil bath, quenched in ice to stop the reaction, and filtered with a 0.2 μm filter (Fisher Scientific).

Quantification of the liquid products was achieved using high-performance liquid chromatography (HPLC, Waters Alliance Instruments e2695), equipped with a refractive index (RI) detector and a photodiode array (PDA) detector. Sugars were separated using a Biorad HPX87C column at 348 K with HPLC-grade water flowing at 0.5 mL min^{-1} as the mobile phase. Acid byproducts and HMF were separated using a Biorad HPX87H column heated to 323 K with 5 mM sulfuric acid flowing at 0.5 mL min^{-1} as the mobile phase.

Results and discussion

Model-predicted $AlCl_3$ speciation in aqueous media

In aqueous media, $AlCl_3$ dissociates to form metal cations. These cations are solvated by water, forming complexes, such as $[Al(H_2O)_6]^{3+}$, which can be further hydrolyzed, as shown in eqn (1).[15,16,27]

$$[Al(H_2O)_6]^{3+} + xH_2O \leftrightarrow [Al(H_2O)_{6-x}(OH)_x]^{(3-x)+} + xH_3O^+ \quad (1)$$

The main species predicted using the OLI software *vs.* HCl concentration include the hexa-aqua species, $[Al(H_2O)_6]^{3+}$, the stable, crystalline solid form of aluminum hydroxide, called boehmite, AlO(OH), and the mono- and di-hydroxy species, $[Al(H_2O)_5(OH)]^{2+}$ and $[Al(H_2O)_4(OH)_2]^{1+}$, respectively (Fig. 1 and Scheme 2). The cations are represented as Al^{3+}, $AlOH^{2+}$, and $Al(OH)_2{}^{1+}$ (for simplicity).

With increasing HCl concentration, the Al^{3+} concentration increases monotonically, and that of AlO(OH) decreases monotonically, whereas the concentrations of $Al(OH)^{2+}$ and $Al(OH)_2{}^{1+}$ exhibit volcano-like curves with peaks at intermediate HCl concentrations. At low HCl concentrations, the concentrations of $Al(OH)^{2+}$ and $Al(OH)_2{}^{1+}$ increase as the pH drops at the expense of the solid. The distribution of aluminum species at high HCl concentrations can be rationalized by Le Chatelier's principle, where an increase in H^+ concentration shifts the thermodynamic equilibrium to the left in eqn (1), suppressing

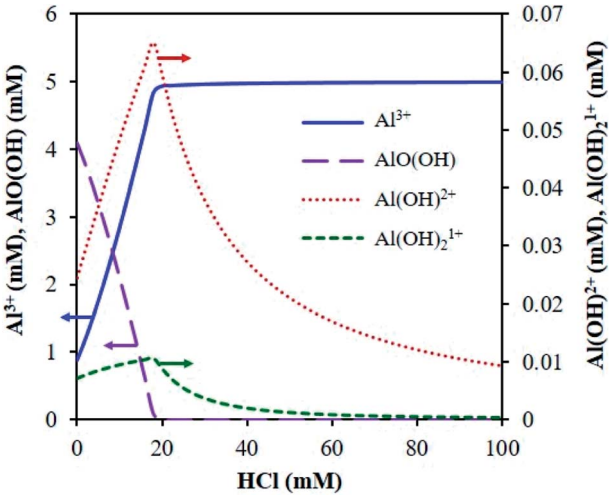

Fig. 1 Distribution of $AlCl_3$ speciation (5 mM $AlCl_3$) at reaction temperature (413 K), calculated using the OLI software.

the formation of the hydrolyzed aluminum species and increasing the concentration of Al^{3+}. The dominance of Al^{3+} species at high acid concentrations has been reported before.[3,15] In addition, the prediction of solid boehmite is consistent with Hem *et al.*'s findings, which demonstrated that heating aqueous aluminum results in the formation of boehmite, whose structure was confirmed by X-ray diffraction (XRD).[28] To our knowledge, the concentrations of the hydrolyzed aluminum species have not been quantified; however, Mesmer *et al.* determined the hydrolyzed species are most significant at relatively low concentrations of aluminum (*e.g.*, ≤10 mM),[29] as considered here. The model predicts the hydrolyzed species' concentrations increase with an increase in solution temperature, which is expected given that aluminum hydrolysis is endothermic (Fig. S3†).[27] Qualitatively, the results remain similar when temperature changes.

Equilibration of $AlCl_3$–HCl catalyst solutions

Next, we investigated the time necessary for the $AlCl_3$–HCl catalyst solutions to reach equilibrium. Equilibration allows formation of the various aluminum species[30] and thus proper comparison between the experimentally measured and predicted speciation,[26] and ensures quasi-equilibrated speciation during short reaction times to enable kinetic analysis (which otherwise can be influenced by varying speciation during kinetics measurements). Different approaches have been employed in prior work to determine the time necessary for equilibrium. Frink *et al.* measured the pH of aluminum salt solutions as a function of time and temperature (298 K and 313 K) upon cooling (*ex situ*).[30] Hem *et al.* performed measurements of the pH together with quantification of polymeric and solid aluminum.[28] Since OLI predictions indicate the formation of solid aluminum, we measure pH and solids. The catalyst solutions were preheated at reaction temperature for 24 h, and the pH was obtained *in situ* and *ex situ*; not a noticeable difference between *in situ* and *ex situ* pH measurements was found (see Fig. 2 at 363 K and Fig. S4† for measurements at 303 K and 413

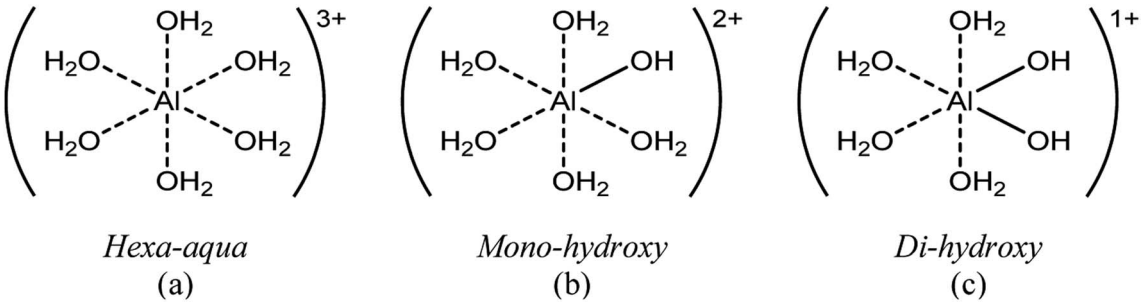

Scheme 2 Al(III) ions generated from the dissolution of $AlCl_3$ in aqueous media.

K). The irreversible pH behavior observed upon cooling is most likely due to the formation of stable solid aluminum species. Thereafter, we present only *ex situ* pH data. The solid was quantified through ultrafiltration followed by ICP-MS analysis of the permeate. The difference between the initial amount of aluminum, prior to preheating, and the concentration of aluminum in the permeate was taken as the amount of solid.

Fig. 3a shows the *ex situ* measured pH and Fig. 3b shows the amount of solid as a function of time. The pH initially drops during the first 1 h and then remains approximately unchanged after 8 h, whereas solid formation increases with time and eventually remains constant after 24 h. Fig. 3 indicates multiple time scales whereby solids form slowly compared to equilibration of small species. Hsu proposed the solid results from an intermediate polymeric species,[14] which forms within the first hour of heating, and, in combination with the formation of the hydrolyzed species, results in the formation of H^+, which decreases the pH. As time increases, the polymeric species undergo nucleation to form stable solid species, such as boehmite.[14] This nucleation and/or subsequent growth is slow, given the number of particles continue to increase for 24 h. DLS measurements further indicate the formation of nanoparticles and provide the average particle growth as a function of time (Fig. S5†). The average particle diameter remains constant after 24 h of heating, which is consistent with the time taken for observable solid formation using ultrafiltration/ICP-MS. We observed similar results for samples preheated at 363 K (Fig. S5†). For these samples, solids were present after being heated for 24 h or longer, and their size and amount remained constant thereafter whereas the pH equilibrated faster (Fig. S6†). Therefore, we have decided to preheat our samples for 24 h at reaction temperature for equilibration of aluminum species prior to conducting kinetic experiments.

Direct measurements of $AlCl_3$ speciation

Fig. 4 outlines the methodology to quantify each species. qNMR measurements were performed *in situ* at 363 K and *ex situ* at 413 K due to instrument limitations.

Hexa-aqua aluminum (Al^{3+})

We first quantified the hexa-aqua monomer, Al^{3+}, using ^{27}Al qNMR, at a chemical shift of ~0 ppm.[31] qNMR spectroscopy is non-destructive, quantitative, and uses a low-energy electromagnetic wave, causing an extremely small energy perturbation to the system.[32–34] In addition, the quantitative accuracy of NMR analysis has reached three significant figures.[32–34] Following a similar approach to that of Maki *et al.*,[32] we measured the concentration of Al^{3+} by comparing the qNMR peak areas of experimental samples to an external standard, which consisted of 5 mM $AlCl_3$ and 100 mM HCl. The concentration of HCl in the standard is high to ensure all aluminum is in the form of Al^{3+}, according to Fig. 1. Similar to the pH measurements, it did not make a difference if the Al^{3+} species was quantified *in situ* (Fig. S7 and Table S1†) or *ex situ* (Fig. 5 and Table S2†); both measurements were in reasonable agreement with the speciation model (Fig. 6a). We hypothesize the unaccounted aluminum exists primarily as suspended solids, which are not detect by liquid-phase qNMR.[15]

Solid aluminum

We next quantified the solid aluminum species. Techniques such as dialysis and ultrafiltration are commonly used to separate fine colloidal mineral aluminum and polymeric aluminum species from soluble aluminum.[15] Therefore, we

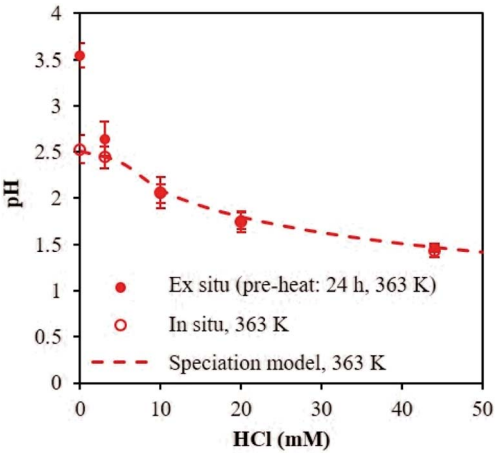

Fig. 2 pH measured *ex situ* (closed circles) or *in situ* (open circles) compared to pH calculated from OLI software (line) at 363 K. Samples contained 5 mM $AlCl_3$. Error bars correspond to 95% confidence interval.

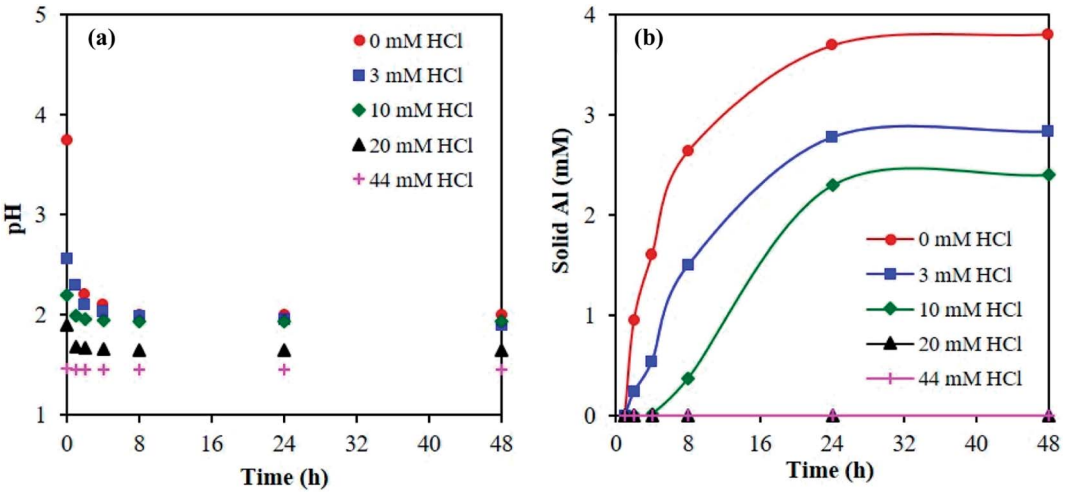

Fig. 3 Determination of equilibrium from (a) pH, measured *ex situ*, and (b) amount of solid formed with time. Samples contained 5 mM $AlCl_3$ and were cooled from 413 K to 303 K.

combined ultrafiltration with DLS and ICP-MS measurements to quantify solid aluminum species in our catalyst solutions. DLS measurements detected the presence of aluminum particles and provided the average particle diameter. This allowed for selection of an ultrafiltration membrane with a pore diameter of 5 nm, significantly less than that detected by DLS (Fig. S8†). The samples then underwent heating and ultrafiltration. ICP-MS determined the concentration of aluminum in the permeate. Our experimentally inferred data are consistent with the calculated amount of solid aluminum (Fig. 6b).

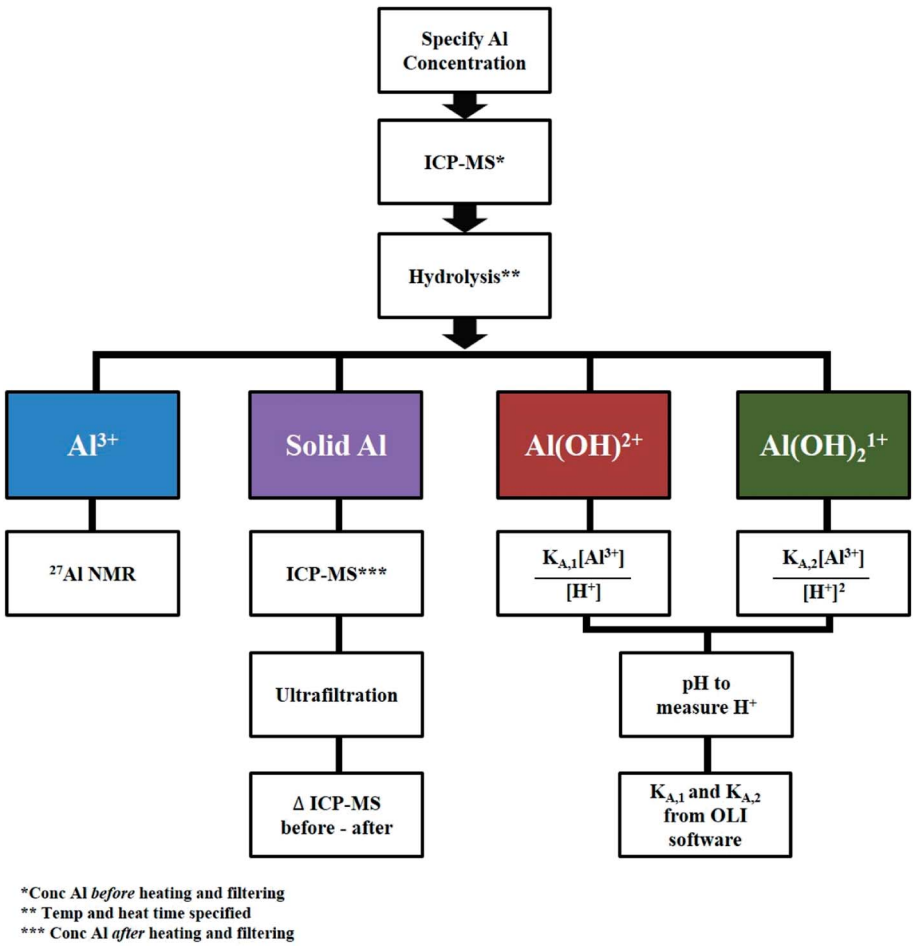

Fig. 4 Methodology to quantify aluminum speciation at specified concentrations of $AlCl_3$ and HCl, temperature, and heating time.

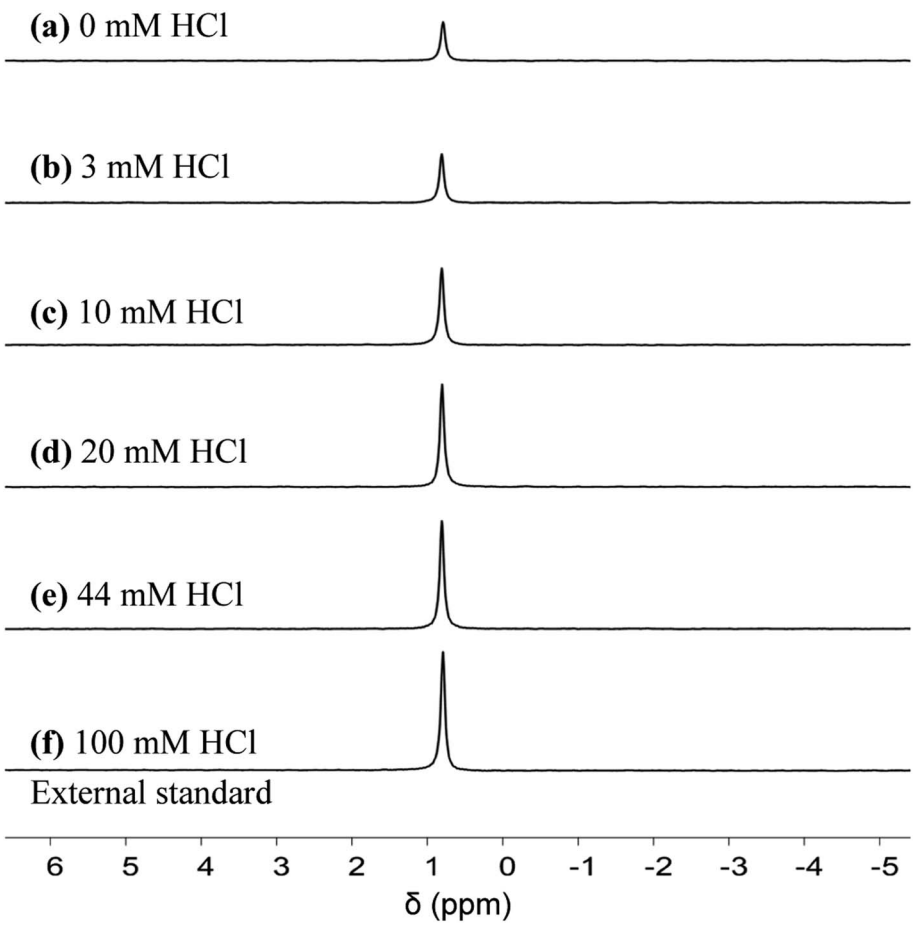

Fig. 5 ^{27}Al qNMR spectra for Al^{3+}. Experimental conditions: preheat 413 K for 24 h, 5 mM $AlCl_3$. qNMR measurements obtained upon cooling to 303 K.

Hydrolyzed monomers ($AlOH^{2+}$ and $Al(OH)_2^{1+}$)

The low concentration and rapid proton exchange associated with the hydrolyzed species make them difficult to observe experimentally.[27] Therefore, we deduced their concentration through the fundamental equilibrium relation (Tables S3 and S4†). This required the Al^{3+} and H^+ concentrations and the acid dissociation constants ($K_{A,1}$ and $K_{A,2}$). The Al^{3+} and H^+ concentrations were obtained by qNMR and pH measurements, respectively. The acid dissociation constants were obtained from the OLI software (Tables S3 and S4†). The experimentally estimated mono- and di-hydrolyzed concentrations exhibit the same volcano-like behavior predicted by the OLI software as a function of HCl concentration, as shown in Fig. 6c and d, respectively.

Glucose conversion and catalytically active species in equilibrated catalyst solution

A series of kinetic experiments with glucose added to preheated catalyst solutions containing $AlCl_3$ and HCl were performed. The initial rates of glucose isomerization were obtained by fitting the glucose concentration profiles at low conversions ($\leq$15%) with a first-order rate expression, where fructose was the main product observed (Fig. S9 and S10†). Fig. 7 shows these rates as a function of HCl concentration.

Interestingly, with increasing HCl, the glucose conversion rate exhibits a trend that is qualitatively consistent with the $Al(OH)^{2+}$ and $Al(OH)_2^{1+}$ species' concentrations, shown in Fig. 1 (see Fig. S3† for 363 K data). The slow glucose consumption at low HCl concentrations (before the maximum rate) is congruent with the formation of solid aluminum species, indicating the solid likely hinders glucose conversion. Tang *et al.* observed, when using solid $Al(OH)_3$ as a catalyst, that $Al(OH)_3$ did not effectively catalyze the reaction, and resulted in low glucose conversion (X = 7.8%) and fructose yield (Y_{Fru} = 6.5%) compared to $AlCl_3$ (X = 31.8% and Y_{Fru} = 26.3%) at the same reaction conditions.[9] Similarly, the Al^{3+} species is not likely catalytically active given the reaction rate continues to decrease as the Al^{3+} species concentration increases. The correlation between the estimated glucose consumption rate and the hydrolyzed species strongly indicates that one or both of these $Al(OH)_x^{(3-x)+}$ species may be catalytically active for glucose isomerization. Since the speciation model[26] was developed at conditions different from typical sugar experiments, we used our direct speciation measurements to elucidate the aluminum species.

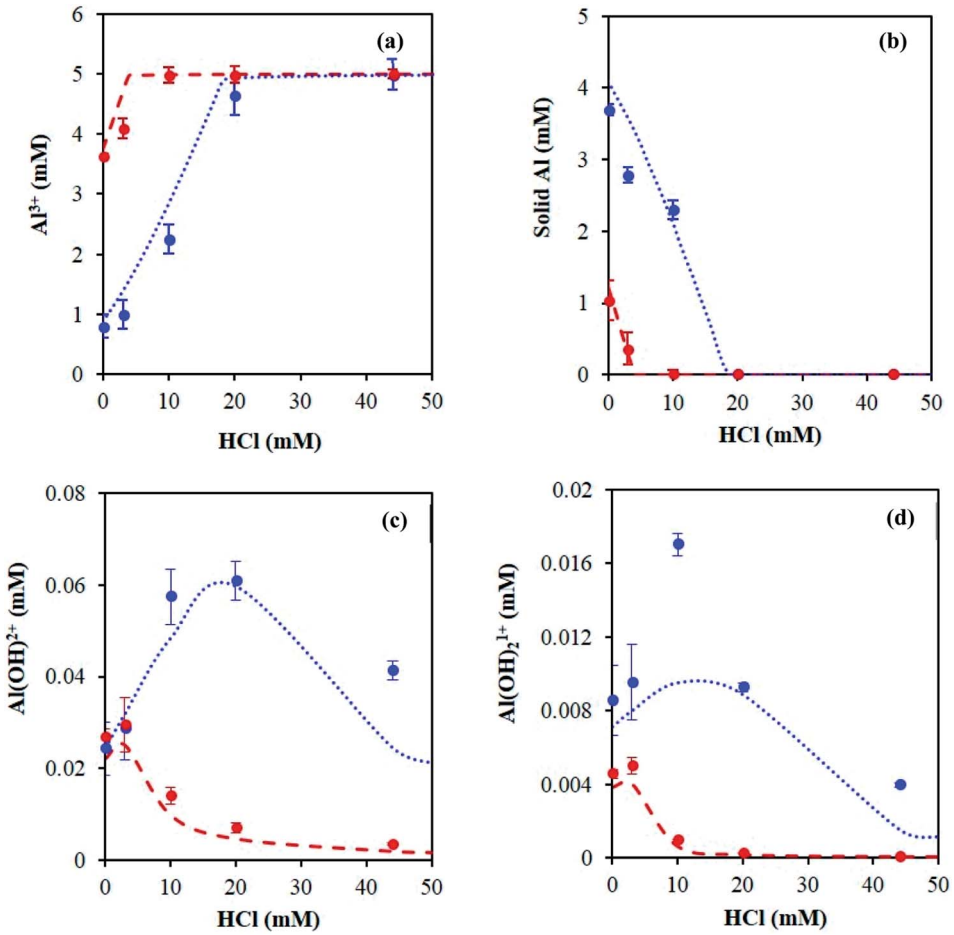

Fig. 6 Aluminum speciation calculated by OLI software at 363 K (red dash lines) and 413 K (blue dotted lines) compared to experimentally inferred species (data represented by red and blue dots). (a) Al^{3+} (measured *in situ* at 363 K and *ex situ* upon cooling from 413 K to 303 K), (b) solid Al (measured *ex situ*), (c) $Al(OH)^{2+}$, and (d) $Al(OH)_2^{1+}$. Experimental samples contained 5 mM $AlCl_3$ and were preheated at specified temperature for 24 h.

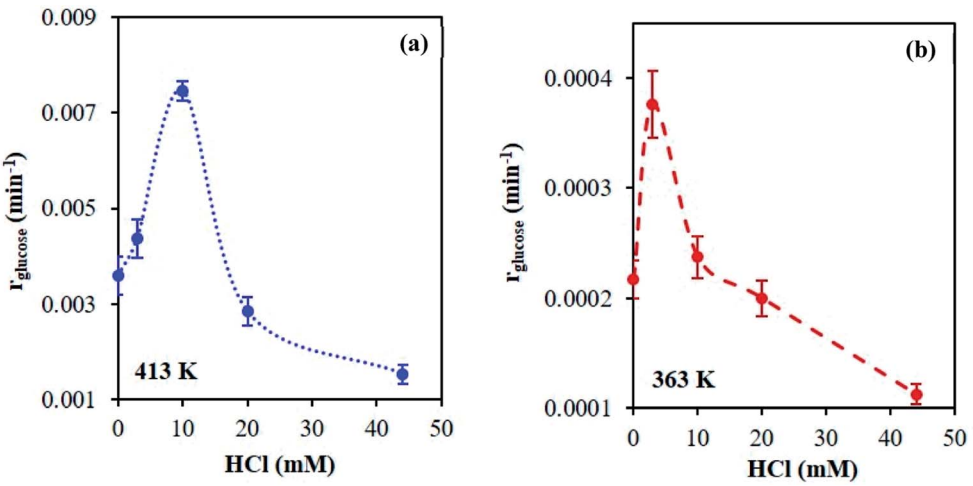

Fig. 7 Effect of HCl on glucose isomerization rate in $AlCl_3$ solutions (5 mM) that have been equilibrated at (a) 413 K and (b) 363 K for 24 h prior to kinetic study. Reaction conditions: glucose 1 wt%, Al to glucose molar ratio 9 : 100.

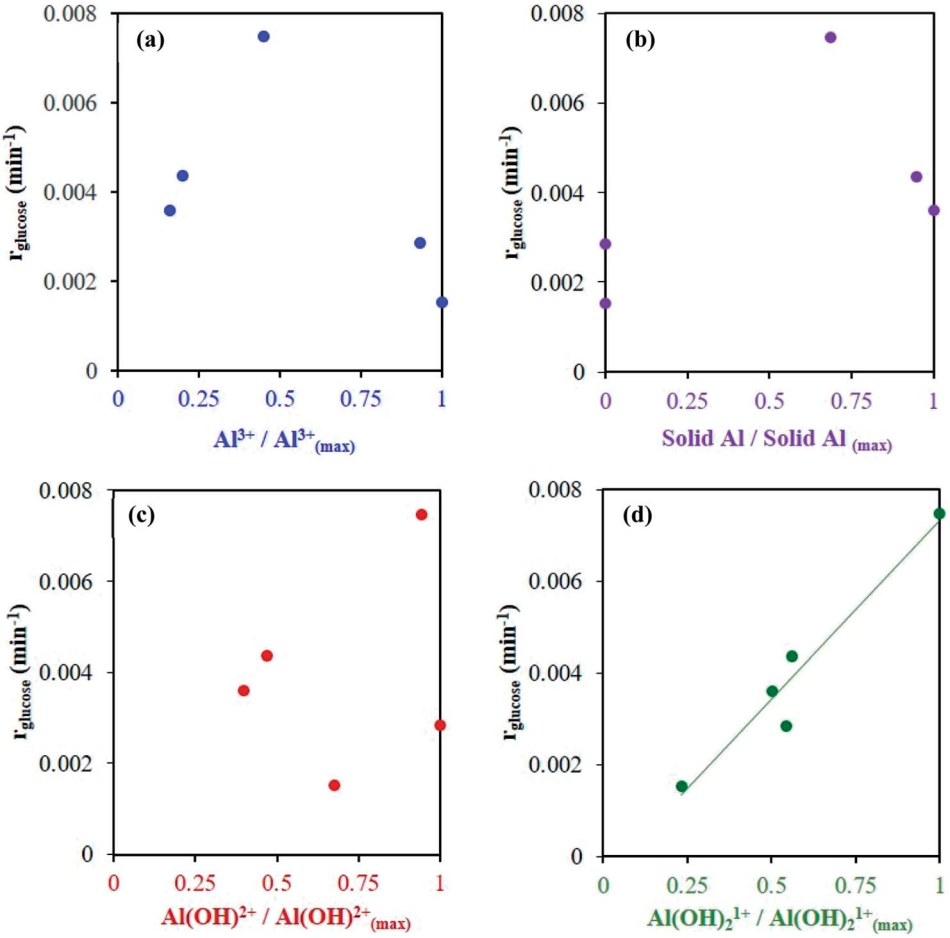

Fig. 8 Glucose conversion as a function of measured Al species' concentrations, normalized to the maximum observed species' concentration (see Table S3† for observed species' concentrations). Catalyst solutions were preheated at 413 K for 24 h prior to kinetic study. Reaction conditions: glucose 1 wt%, Al to glucose molar ratio of 9 : 100, 413 K.

At 413 K, the linear scaling observed between the glucose isomerization rate and the di-hydrolyzed $Al(OH)_2^{1+}$ concentration (Fig. 8) strongly indicates $Al(OH)_2^{1+}$ is the catalytically active species. At 363 K, the low reaction rate, extremely small values of the rate constants and low concentrations of the aluminum species (see Table S4 and Fig. S11†) render our data inconclusive regarding the active species.

Conclusions

We have coupled kinetic studies with direct speciation measurements to elucidate the active species of $AlCl_3$ in glucose to fructose isomerization. Experiments were designed based on insights obtained from modeling the aluminum hydrolysis using the OLI software. We established an experimental protocol to quantify the various aluminum species that employs ^{27}Al qNMR for the hexa-aqua aluminum monomer, ultrafiltration and ICP-MS for the solid, and pH measurements combined with equilibrium relations for the mono- and di-hydroxy aluminum species. We found that speciation reaches equilibrium after heating the catalyst solutions for long times. Linear scaling between the glucose isomerization rate and the speciation measurements at sufficiently high temperatures indicates that the hydrolyzed Al(III) complex $[Al(H_2O)_4(OH)_2]^{1+}$ is the active species in glucose isomerization. This finding supports the hypothesis of Hu and co-workers, who observed $[Al(H_2O)_4(OH)_2]^{1+}$ using ESI-MS/MS.[9] Furthermore, our findings support the idea that the catalytic species responsible for the isomerization exists as a bifunctional Lewis acidic/Brønsted base site.[3] The approach developed here can be applied to study the speciation of other metal halides. For metals not observed by qNMR, such as $CrCl_3$, other spectroscopic techniques, such as ultraviolet visible light spectrometry (UV-Vis), could possibly be employed to study the dominant hexa-aqua species.

Conflicts of interest

There are no conflicts to declare.

Acknowledgements

We acknowledge support from the National Science Foundation under Award No. 1434456. The authors would like to thank Caroline Golt (UD) for performing the ICP-MS measurements, Dr Shi Bai (UD) and Dr Elizabeth McCord (UD) for their assistance with the qNMR method, and John Ruano-Salguero (UD),

Prof. Raul Lobo (UD), and Dr Basudeb Saha (UD) for useful discussions.

References

1 R. J. van Putten, J. C. van der Waal, E. de Jong, C. B. Rasrendra, H. J. Heeres and J. G. de Vries, *Chem. Rev.*, 2013, **113**, 1499–1597.
2 A. Corma, S. Iborra and A. Velty, *Chem. Rev.*, 2007, **107**, 2411–2502.
3 V. Choudhary, A. B. Pinar, R. F. Lobo, D. G. Vlachos and S. I. Sandler, *ChemSusChem*, 2013, **6**, 2369–2376.
4 T. D. Fenn, D. Ringe and G. A. Petsko, *Biochemistry*, 2004, **43**, 6464–6474.
5 R. DiCosimo, J. McAuliffe, A. J. Poulose and G. Bohlmann, *Chem. Soc. Rev.*, 2013, **42**, 6437–6474.
6 S. H. Bhosale, M. B. Rao and V. V. Deshpande, *Microbiol. Rev.*, 1996, **60**, 280–300.
7 M. Moliner, Y. Roman-Leshkov and M. E. Davis, *Proc. Natl. Acad. Sci. U. S. A.*, 2010, **107**, 6164–6168.
8 E. Nikolla, Y. Roman-Leshkov, M. Moliner and M. E. Davis, *ACS Catal.*, 2011, **1**, 408–410.
9 J. Q. Tang, X. W. Guo, L. F. Zhu and C. W. Hu, *ACS Catal.*, 2015, **5**, 5097–5103.
10 T. D. Swift, H. Nguyen, A. Anderko, V. Nikolakis and D. G. Vlachos, *Green Chem.*, 2015, **17**, 4725–4735.
11 Y. J. Pagan-Torres, T. F. Wang, J. M. R. Gallo, B. H. Shanks and J. A. Dumesic, *ACS Catal.*, 2012, **2**, 930–934.
12 V. Choudhary, S. I. Sandler and D. G. Vlachos, *ACS Catal.*, 2012, **2**, 2022–2028.
13 R. Bermejo-Deval, R. S. Assary, E. Nikolla, M. Moliner, Y. Roman-Leshkov, S. J. Hwang, A. Palsdottir, D. Silverman, R. F. Lobo, L. A. Curtiss and M. E. Davis, *Proc. Natl. Acad. Sci. U. S. A.*, 2012, **109**, 9727–9732.
14 P. H. Hsu, *Clays Clay Miner.*, 1988, **36**, 25–30.
15 G. Sposito, *The Environmental Chemistry of Aluminum*, CRC Press Inc., Boca Raton, FL, 1989.
16 C. F. Baes, *The Hydrolysis of Cations*, Krieger Publishing Company, Malabar, FL, 1976.
17 V. Choudhary, S. H. Mushrif, C. Ho, A. Anderko, V. Nikolakis, N. S. Marinkovic, A. I. Frenkel, S. I. Sandler and D. G. Vlachos, *J. Am. Chem. Soc.*, 2013, **135**, 3997–4006.
18 J. Q. Tang, L. F. Zhu, X. Fu, J. H. Dai, X. W. Guo and C. W. Hu, *ACS Catal.*, 2017, **7**, 256–266.
19 I. I. Stewart, *Spectrochim. Acta, Part B*, 1999, **54**, 1649–1695.
20 P. M. Bertsch, R. I. Barnhisel, G. W. Thomas, W. J. Layton and S. L. Smith, *Anal. Chem.*, 1986, **58**, 2583–2585.
21 M. A. Curtin, L. R. Ingalls, A. Campbell and M. James-Pederson, *J. Chem. Educ.*, 2008, **85**, 291–293.
22 B. C. Faust, W. B. Labiosa, K. H. Dai, J. S. Macfall, B. A. Browne, A. A. Ribeiro and D. D. Righter, *Geochim. Cosmochim. Acta*, 1995, **59**, 2651–2661.
23 K. Shafran, O. Deschaume and C. C. Perry, *Adv. Eng. Mater.*, 2004, **6**, 836–839.
24 A. Singhal and K. D. Keefer, *J. Mater. Res.*, 1994, **9**, 1973–1983.
25 P. M. Wang and A. Anderko, *Fluid Phase Equilib.*, 2001, **186**, 103–122.
26 P. M. Wang, A. Anderko and R. D. Young, *Fluid Phase Equilib.*, 2002, **203**, 141–176.
27 C. F. Baes and R. E. Mesmer, *Am. J. Sci.*, 1981, **281**, 935–962.
28 J. D. Hem, *Adv. Chem. Ser.*, 1968, 98–114.
29 R. E. Mesmer and C. F. Baes, *Inorg. Chem.*, 1971, **10**, 2290–2296.
30 C. R. Frink and M. Peech, *Inorg. Chem.*, 1963, **2**, 473–478.
31 J. W. Akitt, *Multinuclear NMR*, Springer, US, New York, 1987.
32 H. Maki, G. Sakata and M. Mizuhata, *Analyst*, 2017, **142**, 1790–1799.
33 F. Malz and H. Jancke, *J. Pharm. Biomed. Anal.*, 2005, **38**, 813–823.
34 G. F. Pauli, B. U. Jaki and D. C. Lankin, *J. Nat. Prod.*, 2005, **68**, 133–149.